Journal of Archaeological Science: Reports 59 (2024) 104789

Contents lists available at ScienceDirect

Journal of Archaeological Science: Reports

journal homepage: www.elsevier.com/locate/jasrep

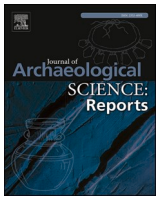

Mercury contamination in ancient water reservoirs at the Maya city of Ucanal, Guatemala

Jean D. Tremblay [a,*], Christina T. Halperin [a], Peter M.J. Douglas [b]

[a] Department of Anthropology, Université de Montréal, Montréal, QC H3T 1N8, Canada
[b] Department of Earth and Planetary Sciences and Geotop Research Center, McGill University, Montréal, QC H3A 0E8, Canada

ARTICLE INFO

Keywords:
Maya
Mercury contamination
Cinnabar
Water reservoirs
Ucanal
Terminal Classic

ABSTRACT

Although the use of mercury in the form of cinnabar (HgS) by the ancient Maya has been widely documented, there are few datasets available to understand potential exposure to mercury from ancient Maya reservoirs. This study analyzed the chemical composition of stratigraphically excavated dried sediments from 3 ancient water reservoirs located in different zones and social contexts at the site of Ucanal, Guatemala, to determine how potential contamination of water reservoirs varied through space and time. High levels of mercury, relative to natural concentrations in soils, were identified throughout the complete temporal sequence and were omnipresent in all three water reservoirs, indicating that mercury contamination may have affected both elite and non-elite sectors of the population. Average total mercury concentrations in the reservoirs' sediments were above 1 μg/g, the toxic effect threshold above which freshwater ecosystem sediments are deemed to be heavily polluted. A sharp increase in mercury was recorded for the Terminal Classic period, when the city reached its apogee, with average concentrations of 3.08 μg/g for Aguada 2, 11.88 μg/g for Aguada 3 and 3.17 μg/g for Piscina 2. Non-reservoir soil samples also show mercury contamination throughout the city core, a situation which would have led to the accumulation of mercury in water reservoirs through its mobilization within the various drainage areas.

1. Introduction

One of the key components to the health of any community, past or present, is the access to clean water sources and environments. Previous geochemical studies of ancient Maya contexts reveal that a range of physical, chemical and biological factors could have affected water sources in the past (Cook et al. 2006, 2022; Lentz et al. 2020; Némery et al. 2016; Tankersley et al. 2020; Waters et al. 2021). Contamination of water by algal blooms or cyanobacteria in antiquity would have been visible to the naked eye and could have triggered corrective actions and/or avoidance behaviors by the Maya, but chemical contamination would have been invisible and was therefore potentially more insidious as it could have remained unnoticed for extended periods, leading to potential harmful health effects.

Although the ancient Maya are known to have had access to elemental mercury, the most common use of mercury was in its form as cinnabar (mercury sulfide: HgS) (Cook et al. 2022; Couoh 2015; Lentz et al. 2020; Pendergast 1982; Quintana et al. 2015; Vandenabeele et al. 2005). Cinnabar was used throughout the ancient Maya world from the early Preclassic to the Postclassic periods in burial rituals (Cervini-Silva et al. 2013, 2018), employed as pigments used to paint buildings and as decorative coloring for luxury ceramics, engraved bone objects, carved stone ornaments and figurines, and as ritual offerings in themselves (Miller 2019:162,192; Rice 2015:160; Sharer et al. 2006:232,349) (Fig. 1). It is believed that the Maya used this inorganic substance due to its intense red color associated with blood and therefore to death and rebirth, an important part of Maya cosmology (Coe and Houston 2015; Miller 2019; Miller and Taube 1993). It differs from other red mineral pigments, such as those deriving from iron oxides, in its purplish shades of red (Houston 2009).

Despite the extensive evidence for the use of mercury-based materials among Maya peoples, few studies have addressed the potentially toxic health effects such materials may have posed through the measurement of mercury concentrations in sediments from ancient Maya cities (Cook et al. 2022; Lentz et al. 2020). Exposure to mercury can occur through inhalation, skin contact or by ingestion of contaminated food, soils, or water (ATSDR 2022). Mercury consensus-based sediment quality guidelines for fresh water ecosystems have been published by

* Corresponding author.
E-mail address: jean.tremblay.2@umontreal.ca (J.D. Tremblay).

https://doi.org/10.1016/j.jasrep.2024.104789
Received 8 April 2024; Received in revised form 26 July 2024; Accepted 22 September 2024
Available online 1 October 2024

MacDonald et al. (2000), and initial chemical research on sediment samples from sites throughout the Maya Lowlands suggest that mercury levels were quite high, and in some cases, exceeded the toxic effect threshold (TET) of 1 μg g^{-1}, the level above which sediments are deemed to be heavily polluted (Cook et al. 2022). Of particular significance are the samples from three water reservoirs at Tikal, in which some samples from the Late and Terminal Classic periods possessed extremely high Hg concentrations exceeding ten times the TET (Lentz et al. 2020). These concentrations are too high to have accumulated naturally, such as through volcanic eruptions. Several studies have reported mercury concentrations from stratovolcano eruptions, although these concentrations were in the low ng/g range (Battistel et al. 2018; Kotra et al. 1983; Kushner et al. 2023:8).

This study expands our understanding of anthropomorphic mercury contamination through the chemical analysis of dried sediments from three water reservoirs located in the ancient Maya city of Ucanal, Petén, Guatemala. It investigates the potential exposure of mercury in different sectors of the city through the sampling of three reservoirs with water catchments from elite residential, middle-and low-status residential, and a mixed zone of public ceremonial and residential buildings of multiple statuses as well as comparative sampling of non-reservoir contexts. It also assesses the changes in mercury concentrations over the course of the settlement and political history of the site through the systematic stratigraphic sampling of the reservoirs and the chronological dating of these contexts through a combination of ceramic and AMS radiocarbon dating.

2. Geological and archaeological context

2.1. Mercury geochemistry

Mercury is a natural component of soils. Worldwide, the average total mercury concentrations in pristine soils are in the order of 0.08 μg g^{-1} (ATSDR 2022; Gonzalez-Raymat et al. 2017), but modern contaminated soils impacted by anthropic activities can reach concentrations as high as hundreds of μg g^{-1} (Kulikova et al. 2019). Its natural biogeochemical cycle is characterized by the degassing of the element from soils or surfaces, its deposition to soils or water bodies and its adsorption /absorption to humic particulate matter (ATSDR 2022; Bank 2012; Canada Environment and Climate Change Canada 2016; Hauser-Davis et al. 2023). In particular, the mining and/or the concentrated use of mercury from cinnabar has the potential to contaminate the surrounding environments either through weathering, direct inputs and/or run-off. Once introduced into the environment, it can gradually accumulate in soils and sediments found in natural or human-made cavities such as water reservoirs. Mercury entering Ucanal's environment would have been mobilized with the potential to accumulate in water pools associated to various drainage areas of the city.

Mercury speciation determines its original fate and pathway into the environment (Bank 2012; Canada Environment and Climate Change Canada 2016; Hauser-Davis et al. 2023). The redox chemistry of mercury at the interface of air and surfaces plays an important role in the deposition and evasion processes of this chemical. In freshwater environments, such as ancient water reservoirs, photoreduction of Hg^{2+} to Hg^0 (dissolved gaseous mercury) can favor evasion (Ferrara et al. 2003; Liu et al. 2012) but mercury reduction and oxidation in water systems would have happened simultaneously and at very similar rates with equilibrium potentially reached rapidly (Whalin and Mason 2006). Ancient water surfaces were likely oxidizing environments while the accumulating sediments were probably reducing. Therefore, in water and/or soils, mercury has the potential to evade or to combine with various ions and the final form in which it exists ultimately depends on the singular pathway it has followed. Since human-made reservoirs are very shallow environments relative to lakes, there is a low potential for methylation of mercury in the hypolimnion of those structures (Noh et al. 2018; Suchanek et al. 2008). Total mercury in accumulated sediments (Σ Hg elemental + Hg_{inorg} + Hg_{org}) is therefore a good indicator of direct input and/or supernatant water contamination by this element (Kocman et al. 2011).

Dill (2010) reported that cinnabar, as a hydrothermal mineral, could be associated with three possible geologic settings: a) Magmatic (associated to intrusions) zone of subduction and volcanic arcs, b) structure bound (associated with faults) due to the metamorphism of sedimentary and volcanic sequences following fault development, and c) sedimentary, when mercury rich hydrothermal fluids mineralize sediments and form mercury deposits. A few cinnabar deposits are documented in Mexico (Ávila et al. 2014; Cook et al. 2022; Gallagher and Perez Siliceo 1948; Martínez-Trinidad et al. 2013), while Pendergast (1982:533–534)

Fig. 1. Cinnabar found on artifacts from Ucanal, Guatemala: (a) crushed cinnabar pigment on the interior of a utilitarian ceramic vessel (Cambio Unslipped type) and likely as a receptacle for pigment preparation, it was recovered intermixed with materials from a Late Classic bone tool production workshop in elite residential Group J (UCA1B-12-8-1322); (b) jade ornament (UC-PV-042) from a royal burial deposit, Burial 20-1 (photographs by C. Halperin).

indicated that the ancient Maya potentially collected cinnabar from Early Cretaceous formations near Lake Atitlán (see also Rytuba 2003) and from Late Cretaceous formations in western Honduras (see also Gorokhovich et al. 2020). There is no known natural cinnabar deposit in the Petén, Guatemala, nor is its geology conductive to such deposits. As such, it is possible that cinnabar found in Petén was imported through trade from either of these potential source locations.

Volcanic eruptions are common in Central America, and dry and wet deposition of natural non-anthropogenic mercury can affect the local accumulation of mercury, although these often occur at relatively low levels. Concentrations of mercury in volcanic ash, however, can vary significantly based on the specific volcano, the characteristics of the eruption, and distance from the eruption. Kushner et al. (2023) reported on volcanic ash mercury content from the eruptions of 3 andesitic stratovolcanoes: Mount Spurr with an average Hg concentration measured at 77.6 ng g^{-1} with samples collected between 5 and 378 km; Augustine Volcano ash with samples collected at a distance of 1 to 85 km, which had a mean Hg concentration of 7.2 ng g^{-1}; and Redoubt Volcano with samples collected between 3 to 333 km with an average Hg concentration of 22.8 ng g^{-1}. They also report on 12 other volcanos. All Hg ashes concentrations were in the ng g^{-1} range with the majority at 10 ng g^{-1} or lower (Kushner et al. 2023:8). Measurements of Hg directly in the plume of the 1982 eruption of another andesitic stratovolcano, El Chichón, Mexico have been documented to be in the ppt range (Kotra et al. 1983). Ashes of this particular event did not reach Ucanal (Espíndola et al. 2000:91), and plume Hg concentrations were not indicative of potential high dry/wet Hg deposition in the greater Maya Lowlands.

Ucanal is in the southern Petén region of Guatemala, which is characterized by a series of rivers that drain from the Highland regions from the south and southeast. The climate of this region is a mix of *Aw* and *Am* Köppen climate classifications with dry and wet seasons along with tropical monsoons (Christopherson 2009; Folan 1983; Wahl et al. 2007). Over the long term, the area can see wide interannual

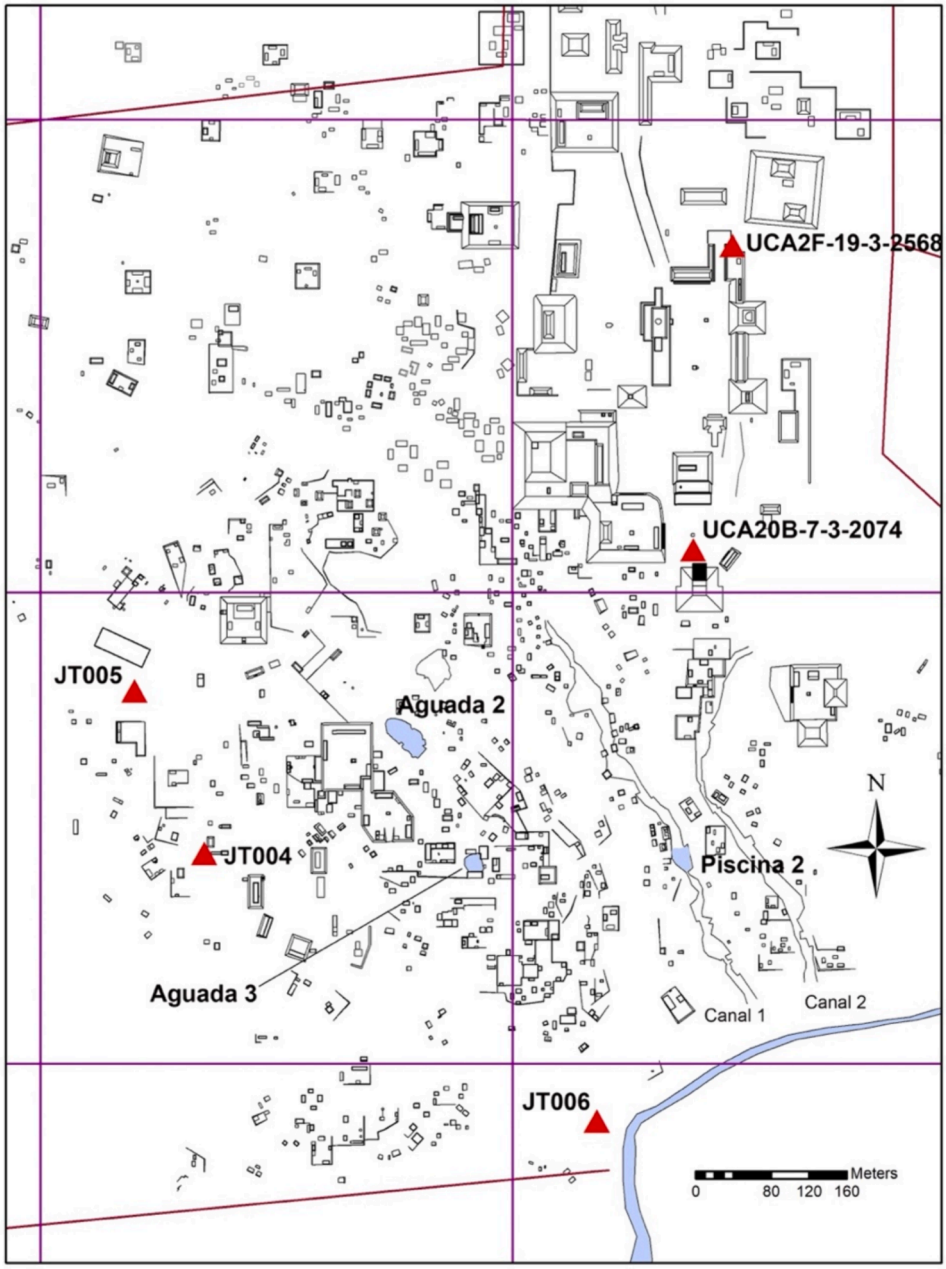

Fig. 2. Map of part of the city of Ucanal showing the locations of Aguadas 2,3 and Piscina 2, and location of background test samples collected around the city core.

fluctuations in precipitation (Dunning et al. 1998; Gunn et al. 2002) and ensuring access to water in both adequate quality and quantity was crucial to Maya society.

2.2. Archaeology

The archaeological site of Ucanal is located along the Mopan River which originates from the Maya mountains via the Vaca Plateau (Seefeld 2018). Since the river is not known to dry up during the annual dry season, inhabitants of the site would have had regular access to water. Nonetheless, Pre-Columbian peoples regularly constructed water reservoirs, drainage canals, dams, terraces, and other features to more effectively access and manage water resources (Dunning et al. 1999; Lucero 2002; Lucero et al. 2011; Scarborough 1998; Scarborough et al. 2012), even if they were located close to rivers, and the site of Ucanal was no exception. Part of the water infrastructure system at the site of Ucanal included large, monumental-scale reservoirs, smaller reservoirs or water collection zones, and large-scale open-air canals, which were integrated with public plazas, roads, and civic-ceremonial buildings to drain to the Mopan River to prevent flooding and erosion in residential areas of the ancient city (Halperin et al. 2019).

Investigations of Ucanal's water infrastructure systems have been undertaken by the Proyecto Arqueológico Ucanal (PAU), directed by Christina Halperin of the Université de Montréal and Guatemalan archaeologists, Lic. Jose Luis Garrido (2014–2022), and Lic. Carmen Ramos Hérnandez (2023-present). Excavations of reservoirs to date have targeted a large, monumental reservoir, Aguada 2, a small residential reservoir, Aguada 3, and a water reservoir integrated into a larger drainage canal, Piscina 2 of Canal 1 (Fig. 2). Aguada 2 is located at one of the highest elevations of the site and was surrounded primarily by large residential groups interpreted to have been occupied by the city's elite. It had an estimated holding volume of $2.6x10^6$ L and had a water catchment drainage area of 10,919 m^2 (Halperin et al., 2023) (Fig. 3). Although large in size for the site, Aguada 2 is smaller than those at other sites, such as Tikal, whose Temple, Palace and Corriental reservoirs held respectively 27, 74 and 57×10^6 L of water that supported a city located at a significant distance from any river or lake (Scarborough et al. 2012). Aguada 3 is located near a grouping of mid- and small-sized residential groups interpreted to have been of middle status or non-elite status (Halperin et al. 2023a). It had a holding volume estimated at 450 $x10^3$ L associated with a drainage area of 6,057 m^2. Piscina 2 (P2C1) is located at the lower ¼ mark of Canal 1 before its drainage into the Mopan River. The pool serves as a water attenuation tank to slow the flow of water and erosion during the rainy season and as such, it was a dynamic water retention zone with a large drainage area of 158,805 m^2 (Gauthier and Flynn-Arajdal 2024). It was likely accessed for water collection by lower-status non-elite inhabitants since small-sized residences surrounded it. Its water catchment zone, however, includes public ceremonial plaza spaces as well as elite and non-elite residential sectors.

Archaeological research at the site of Ucanal by the Proyecto Atlas Arqueológico de Guatemala, directed by Juan Pedro Laporte, (1998–2000) and the PAU reveals that it was occupied from the Middle Preclassic to Postclassic periods (ca. 800 BCE – 1521 CE) (Halperin et al. 2021; Halperin et al. 2024b; Laporte and Mejía 2002). Although it was likely only a small village during the Middle Preclassic period, it became an important ceremonial center by the Late Preclassic period (ca. 300 BCE – 300 CE) when many of the civic ceremonial zones of the site were built-up for the first time and residential occupation is well-documented. The height of its occupation was during the Late Classic (ca. 600–810 CE) and Terminal Classic periods (ca. 810–950/1000 CE), with a likely small population growth between the Late Classic and Terminal Classic periods. Mapping has revealed that the site was quite extensive at its apogee, with a monumental and residential core of at least 7.5 km^2 and a wider periphery that extended at least to a zone of 26 km^2 straddling both sides of the Mopan River. The public monumental zones include over 12 major public ceremonial complexes, three of which have ballcourts (Halperin et al. 2019, 2021). Based on the number of identified structures (Canuto et al. 2018), the site population is preliminarily estimated to have been between 8,000 and 11,000 people at its peak, although these numbers would be larger with the inclusion of outlying settlement zones.

For much of the Classic period, Ucanal, known as K'anwitznal in glyphic texts, was subordinate to other larger polities, including Tikal, Naranjo, and Caracol (Halperin et al. 2020; Martin 2020). During the

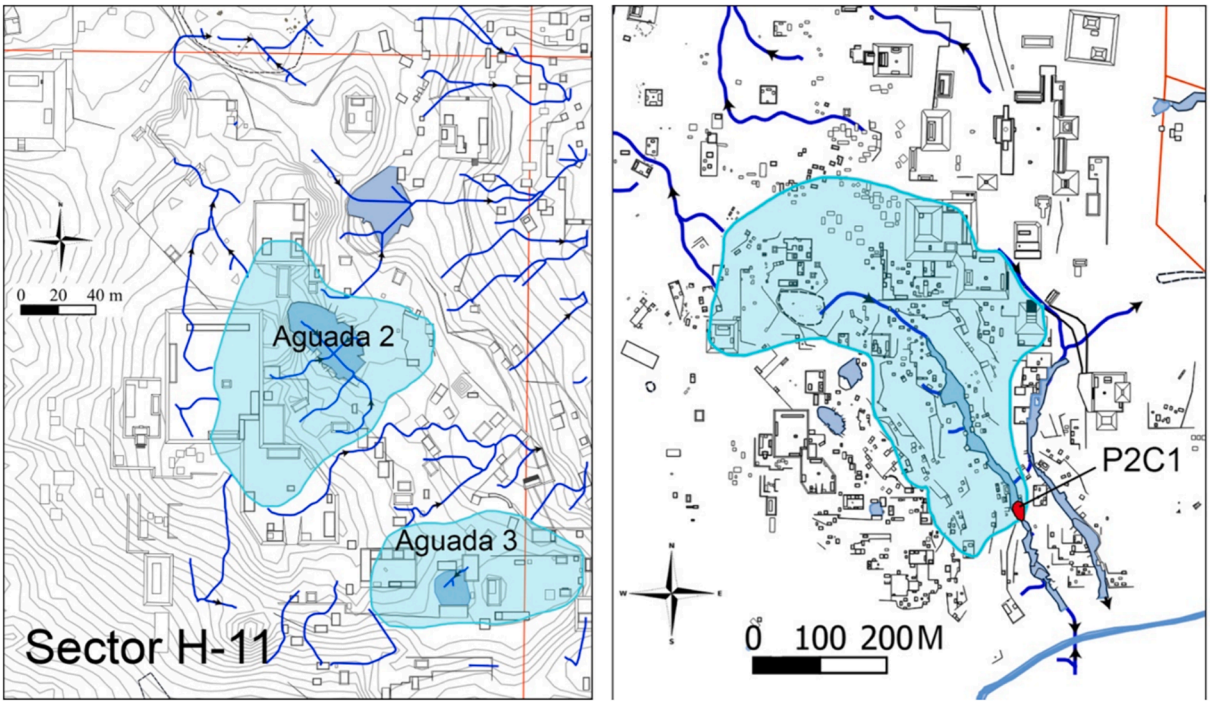

Fig. 3. Map of Aguadas 2, 3 (left) and Piscina 2 (right) with their respective water catchment zones (in blue).

Terminal Classic period, however, the K'anwitznal polity underwent a large-scale renewal: forging alliances with new political entities throughout the Maya Lowlands, undertaking major civic-ceremonial building campaigns in the city's site core, and erecting new monuments throughout the 9th century (Halperin and Garrido 2020; Halperin and Martin 2020). Excavations of three of the city's canals indicate that these water drainage systems were built at the beginning of the Terminal Classic period, helping safeguard residential populations from flooding during monsoons or annual rainy seasons (Halperin et al. 2019). Population, however, diminished significantly during the Postclassic period with no evidence of any major Postclassic building projects, although all excavated groups contained some Postclassic pottery even if in very small amounts (Halperin et al. 2021; Perea 2023).

3. Materials and methods

3.1. Dried sediments sampling

Aguadas 2 and 3 were excavated in 2022 and P2C1 in 2023. Dried sediments (soil samples) were stratigraphically excavated from excavation units located at the center of each reservoir. Excavations followed 10 cm level changes until bedrock. After reaching bedrock, dried sediment samples were taken from a cleaned side of the excavation wall every 10 cm using a stainless steel spatula, working from the bottom layer to the top humic layer of the reservoirs, following current environmental research practices (Keenan et al. 2021, 2022; Köster et al. 2005; Kulikova et al. 2019; Lentz et al. 2020). With a depth of 3.5 m, Aguada 2 recovered samples from 35 distinct levels. Aguada 3 had 12 levels (1.2 m deep), and P2C1 (1.5 m deep) provided 15 levels of dried sediments. To identify potential source zones of mercury contamination in the city and to determine surrounding levels of mercury, 5 extra soil samples were collected: two from excavations in the public, ceremonial sector of the city, two from surface collections (10 cm below the ground surface) of residential zones, and one from surface collection in a zone slightly away from architecture just north of the Mopan River (Fig. 2). Collected dried sediments and carbon (charcoal) samples were placed in sterile Whirl Pak bags, kept at room temperature, and transported to the Earth and Planetary Sciences laboratory at McGill University in Canada at the end of both field seasons. A duplicate of all the samples was kept at the Proyecto Arqueológico Ucanal (PAU) laboratory in Flores, Guatemala, and some samples were split for Quality Assurance and Quality Control (QA/QC) purposes. Upon reception in Canada the samples were freeze dried to remove any water content, weighed, ground and sieved (USA STD Testing Sieve No.8, 2.36 mm). Both coarse and fine fractions were thereafter kept in a −20 °C freezer.

Our study followed standard archaeological procedures whereby samples were not handled under anoxic conditions (Cook et al. 2022; Lentz et al. 2020; Turner et al. 2021; Wells et al. 2000). The dried sediments analyzed were therefore exposed to oxygen while being manipulated. Furthermore, given that the reservoir sediments probably were not covered in water for hundreds of years, they may have experienced oxic conditions long before sampling. The lack of anoxic sampling methods is common to published archaeological studies covering the presence of mercury in ancient Maya sites (Cook et al. 2022; Lentz et al. 2020; Turner et al. 2021; Wells et al. 2000). It is important to keep in mind that redox chemistry occurred throughout the history of sediment accumulation in the 3 reservoirs studied which cover centuries and, in the case of Aguada 2, more than a thousand years. Measuring total mercury in this case was the only means of quantifying the end result of Hg accumulation and evasion, even if this may underestimate the total Hg present at the time of deposition.

3.2. TC, TOC, and pH

We also measured other geochemical parameters, including total carbon (TC), total organic carbon (TOC), and pH, which will be analyzed in detail in a forthcoming article. Here we present a summary of the results that support our analysis of the Hg measurements. Among those, soil pH was measured with an Oakton pH Meter (probe MA918) calibrated with pH 4, 7 and 10 standard solutions. Ten grams of samples were added to 25 ml of 0.01 M $CaCl_2$ solution and mixed for 30 min before measurement. TC and TOC were measured at the Geotop Research Center on Earth Dynamics Light Stable Isotope Geochemistry Laboratory in Montréal, Canada. Measurements were carried out by combustion and separation of elements using a Carlo Erba NC2500 gas chromatograph coupled with a thermal conductivity detector. Considering the high inorganic carbon levels found throughout the sediment columns, sample aliquots for TOC measurements were first treated with a 1 N HCl solution and centrifuged at 4000 rpm for 20 min to remove the supernatant liquid. This process was repeated until all excess $CaCO_3$ was removed as indicated by the absence of CO_2 gas. It was then brought to neutral pH with milli-Q water and freeze-dried (Labconco Freezone 12) prior to measurement.

3.3. Dating of the reservoirs

AMS radiocarbon analyses were conducted at the University of Ottawa in Canada and complemented by ceramic analyses performed at the PAU lab in Flores, Guatemala. For radiocarbon measurements, sample pretreatment techniques, processing and definitions of media codes can be found in (Crann et al. 2017) and (Murseli et al. 2019). Calibration was performed using OxCal v4.4 (Ramsey 2009). Calibrated results are given as a range (or ranges) with associated probabilities (Millard 2014). Ceramic chronologies were established by PAU personnel, led by Miriam Salas, based on regional ceramic type-variety classifications and their ceramic complexes (Gifford 1976; Laporte 2007; Salas et al. 2018). Ceramics were found in all levels of the three reservoirs, providing 100 % chronological coverage (Appendix A).

3.4. Mercury measurements

Total mercury measurements were conducted at the Université de Montréal Biological Sciences laboratory in Canada using a Direct Mercury Analyzer model DMA-80 EVO with thermal decomposition followed by catalytic conversion, amalgamation, and atomic absorption detection. Combustion occurred at 650 °C under O_2 for 90 s with granular catalyst to reduce mercury, and gold column for amalgamation. Absorbance was measured at 253.7 nm with 3 calibration curves (0–2 ng Hg; 2–25 ng Hg and 25–250 ng Hg). The detection limit of the technique was 0.01 ng g^{-1}. Typical sample mass introduced in the analyzer was between 15 and 40 mg of dried sediments. One blank and one known standard were run every 10 samples with auto blank cycles being introduced in the sample run to clean the system following the reading of high mercury concentrations.

3.5. Global data set statistical errors

A total of 62 levels of dried sediments were collected from the 3 reservoirs, of which 8 (13 %) were collected in triplicates for QA/QC: 4 for Aguada 2 (35 levels), and 2 for both Aguada 3 (12 levels) and P2C1 (15 levels). Samples from these levels were split and triplicates were subjected to parallel manipulations and analyses. The global error on our data set was evaluated using three different approaches. First, the standard error was calculated for each QA/QC samples, the average of those errors was computed and simply applied to our data set. This methodology led to a global error for our data set of ±8.3 %. This approach likely underestimated the true error of our data set since the uncertainty for the QA/QC samples which were measured in triplicates is lower than the uncertainty for the remaining samples measured only once. An alternate and more conservative error determination is to establish the global error by dividing the average standard deviation (SD) for our QA/QC samples by the average value of all concentrations

in our data set as proposed by Polissar and D'Andrea (2014:152,155). This approach led to a global error of ±14.3 %. Finally, we calculated the average variation coefficient for our QA/QC samples and extrapolated it to our data set as discussed by Reed et al. (Reed et al. 2002:1238). This approach led to a very similar global error of ±14.5 %. For this study, considering the size of our data set and the size of our QA/QC, we opted for the most conservative approach of error determination and established our global error to be at ±14.5 %. Complete data from QA/QC samples and subsequent global error calculations tables can be found in Appendix B.

4. Results

All levels of dried sediments in the 3 reservoirs studied as well as samples collected in the city core but outside the drainage areas of our reservoirs registered the presence of mercury. Various benchmarks allow us to partially qualify our results. They include:

Benchmark 1, the reported worldwide pristine soil mercury concentration average which sits at 0.08 μg g^{-1} (ATSDR 2022; Gonzalez-Raymat et al. 2017);

Benchmark 2, the Canadian environmental quality guidelines for mercury in freshwater sediments for the protection of aquatic life of 0.14 μg g^{-1}, the level above which statistically probable deleterious effects can occur (Gaudet et al. 1995);

Benchmark 3, the toxic effect threshold (TET) above which freshwater ecosystems sediments are deemed to be heavily polluted which is reported to be at 1.0 μg g^{-1}, the level above which adverse effects on sediments dwelling organisms are recorded (MacDonald et al. 2000) and;

Benchmark 4, the Canadian soils contamination guideline for agricultural and residential land use of 6.6 μg g^{-1} (CCME 2007; Environment Canada 2010).

Mercury concentration distribution with depth tables for Aguadas 2, 3, and P2C1 as well as total mercury results from soil samples collected within the city core outside the drainage areas of our reservoirs can be found in Appendix C. For these tables, the average measured concentrations of the QA/QC triplicates were attributed to the corresponding levels. All dried sediment samples collected in the 3 reservoirs had very high calcium carbonate content. Total carbon was in the 9–11 % range while total organic carbon readings were typically in the 1–2 % range except those from the humic zone (top 30 cm) which were typically in the 4–8 % range. Most samples had a coarse fraction (> 2.36 mm) in the 20–30 % range with some exceptions which will be discussed below. pH readings were between 7.3 and 7.9 indicative of a slightly alkaline environment regardless of reservoirs and depth.

4.1. Aguada 2

For Aguada 2, all 35 levels exceeded Benchmark 2, and 12 levels exceeded Benchmark 3 including all levels dating to the Terminal Classic Period (Fig. 4). While Middle Preclassic ceramics were found in the lowest levels of Aguada 2, it is likely that the construction of this aguada

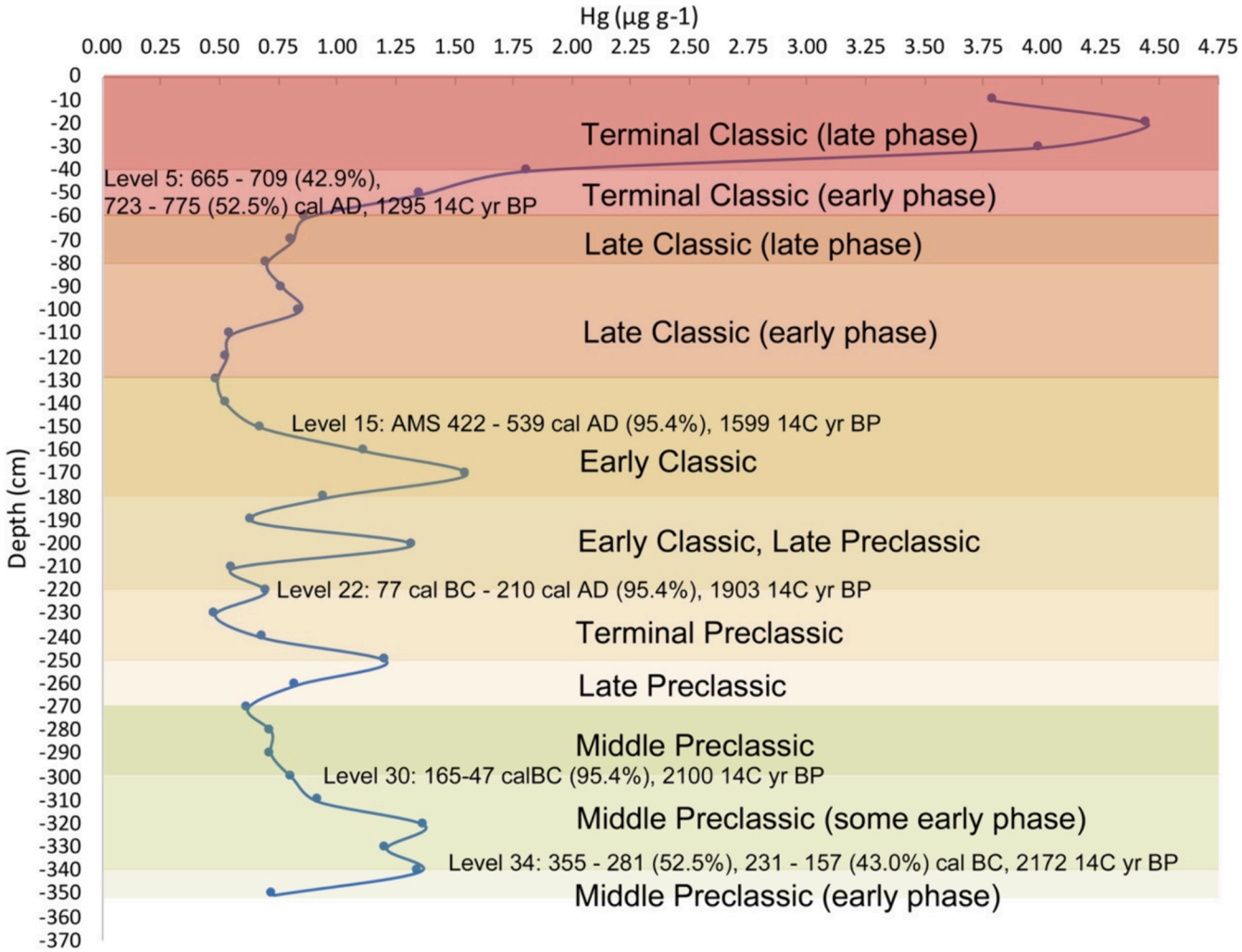

Fig. 4. Aguada 2 total mercury concentrations profile by depth with ceramic chronologies (color blocks) and AMS radiocarbon dating (Appendices B and C).

first began in earnest during the Late Preclassic period according to the radiocarbon dating. Middle Preclassic ceramic material mixed with later ceramics were deposited through erosion at the bottom of the Aguada along with soils from the Late Preclassic. Spanning from at least the Late Preclassic to the Terminal Classic periods, Aguada 2 has the longest chronology of the 3 reservoirs. Although the 3.5 m sediment accumulation at the bottom of the reservoir is uninterrupted for ca.1000 years, we cannot exclude the possibility that the reservoir could have become dry from time to time during extended low precipitation periods. Regardless, we found no signs of sediment manipulations nor renovation efforts at the bottom of the reservoir after the Late Preclassic period (Cruz Gómez and Quezada 2023). Granulometry shows little fluctuation in the coarse fraction of our soil samples throughout the sedimentation sequence with an average of 23.0 % (SD of 6.5 (N = 35)) of the collected material larger than 2.36 mm. With the global error on our mercury readings being 14.5 %, we are limited in drawing broad conclusions about mercury concentrations fluctuations from dry sediment layers with the exclusion of the Terminal Classic associated levels, which represented a significant change in concentrations. The average total mercury concentrations detected from levels 6 to 35 in Aguada 2 was 0.84 μg g^{-1} with a standard deviation of 0.29 (N = 30). We found mercury concentrations falling outside SD variations in 5 levels all exceeding TET, 2 of which are in the Early Classic (levels 17 and 20: 1.55 and 1.32 μg g^{-1}) and 3 at the bottom of the reservoir in layers associated with Late Preclassic soils (levels 32, 33 and 34: 1.37, 1.21, 1.35 μg g^{-1}), a time when Ucanal became an important ceremonial center. Excluding those readings which fall outside statistical fluctuations, concentrations remained relatively constant from the construction of the reservoir all the way to the Late Classic period. A sharp increase in mercury concentrations (up by a factor of 360 %) is recorded in the Terminal Classic period when the average total mercury reached 3.02 μg g^{-1}.

4.2. Aguada 3

Aguada 3 is located near residential Group 151 occupied by non-elite inhabitants (Halperin, Chalifour, et al. 2024; Halperin et al. 2023). It sits 150 m southeast of Aguada 2. For this reservoir, all but one of the 12 levels exceeded Benchmark 2, 7 exceeded Benchmark 3, and 5 had levels exceeding Benchmark 4 (Fig. 5). At 1.2 m deep, Aguada 3 is a much shallower reservoir than Aguada 2. This reservoir appears to have been constructed during the end of the Late Classic period or beginning of the Terminal Classic period. Levels 7–8 comprised a compact construction fill and levels 9–12 comprised a compact *sascab* stratum (Halperin et al. 2023b:135–136). Correspondingly, soil analysis of these lower levels was characterized by powdery cream-colored matrix containing large quantities of calcium carbonate powder mixed with 40–60 % coarse fraction composed of limestone. AMS radiocarbon dating of the compact *sascab* in level 11 corresponds to the Late Classic period, and Late Classic ceramics dominated levels 7–12 even though mixed with those of earlier periods. The average total mercury concentration for these lower levels was 0.36 μg g^{-1}. The upper 6 levels dated, based on ceramic analysis, to the Terminal Classic period and represented the accumulation of soil through erosion. The average mercury concentration associated with Terminal Classic levels was 11.88 μg g^{-1} with a peak concentration of 16.91 μg g^{-1} at level 3, the highest concentration recorded in our study. As such, the average mercury concentration increased by more than 3000 % between the Late and Terminal Classic periods.

4.3. Piscina 2 of Canal 1

For P2C1, all excavated levels exceeded Benchmark 2, and 11 exceeded Benchmark 3 (Fig. 6). The larger canal system, including P2C1, was constructed at the beginning of the Terminal Classic period (Halperin et al. 2019), but the P2C1 reservoir itself may have been a zone of soil and water accumulation dating back to earlier periods. Although a homogenous and compact fill level was not identified,

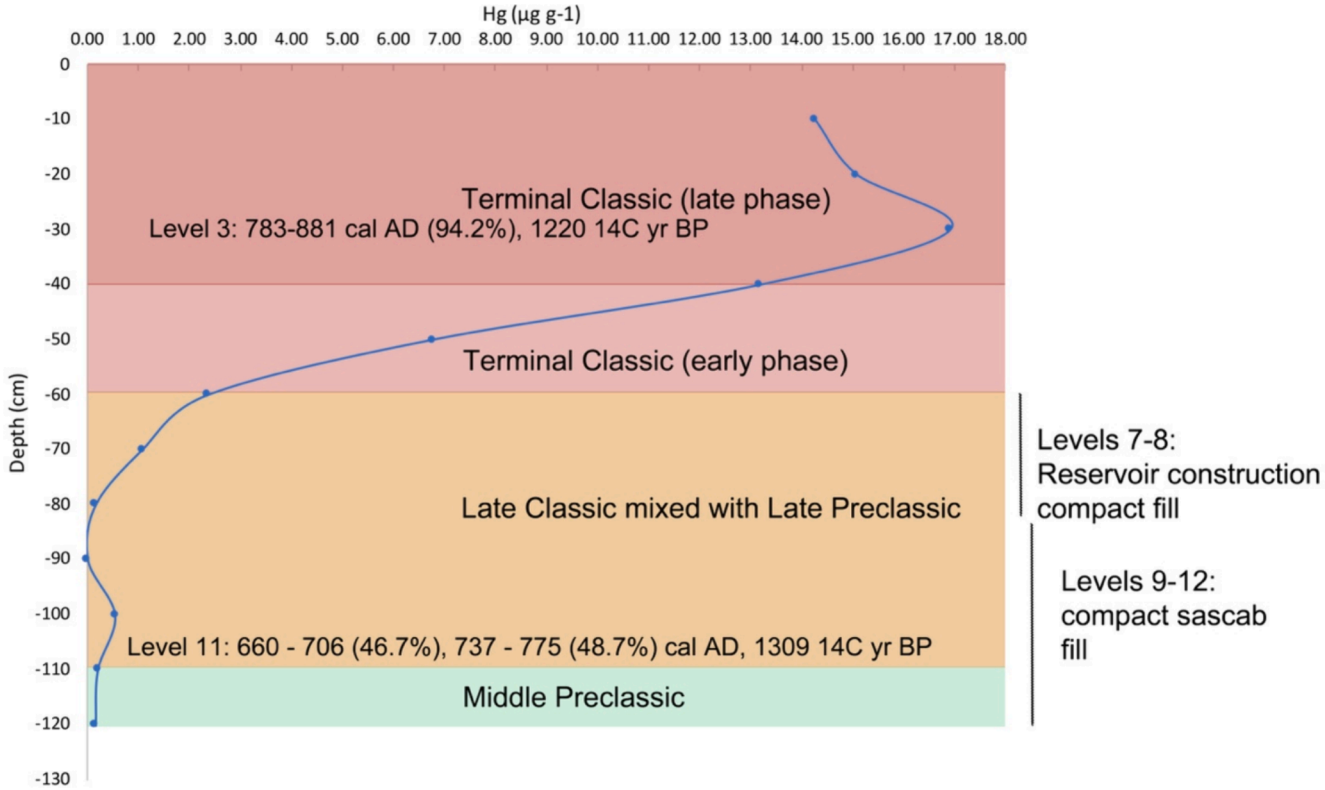

Fig. 5. Aguada 3 total mercury concentrations profile by depth with ceramic chronologies (color blocks) and AMS radiocarbon dating (Appendices B and C).

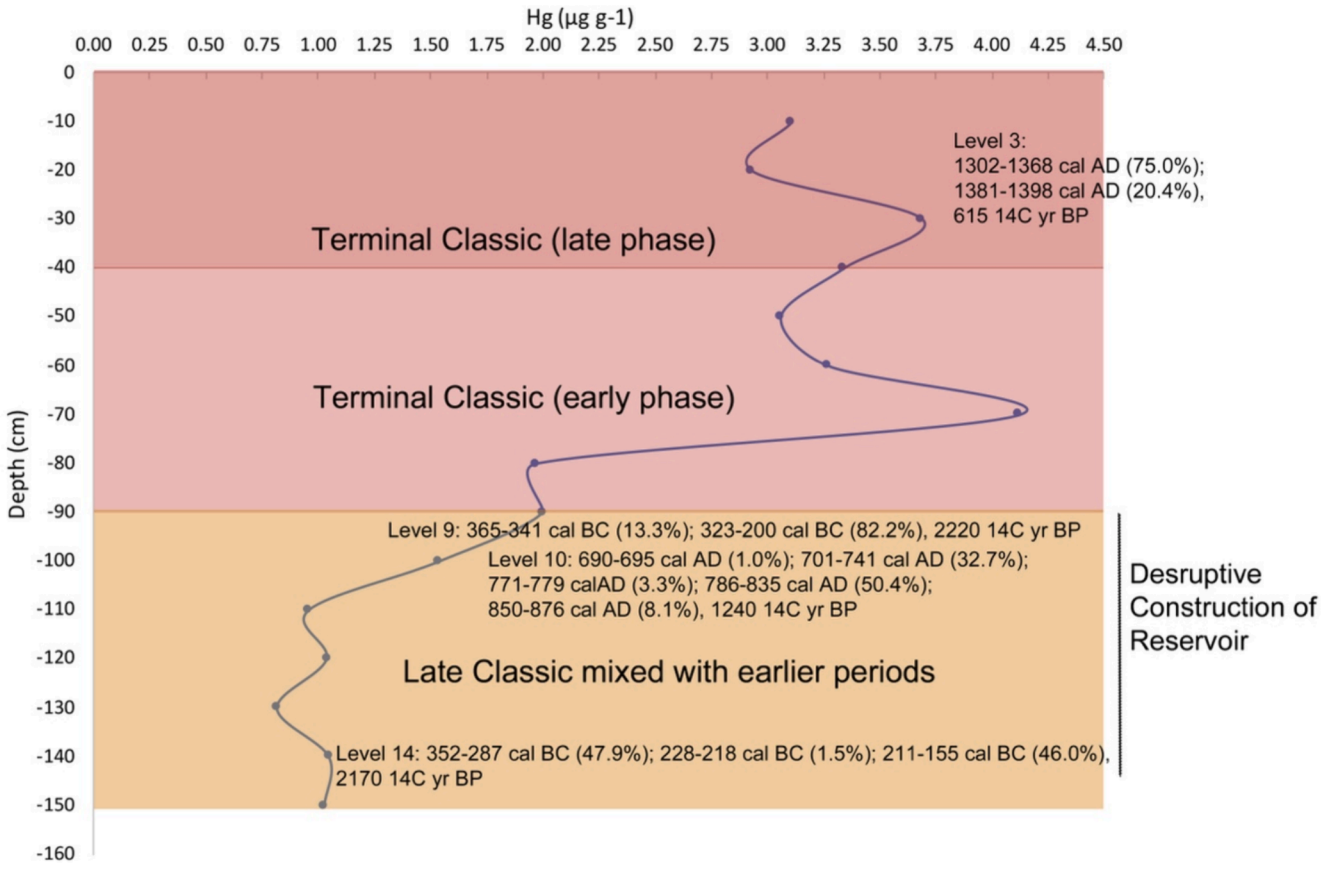

Fig. 6. Piscina 2 of Canal 1 mercury concentrations profile by depth with ceramic chronologies (color blocks) and AMS radiocarbon dating (Appendices B and C).

evidence of the reservoir's construction appears most evident in the lowest levels, levels 9–15, which contained ceramics of mixed time periods (Gauthier and Flynn-Arajdal 2024). Levels 10–15 contained ceramics primarily dating to the Late Preclassic and Early Classic periods. The lack of levels with high concentrations of Late Classic ceramics is noteworthy since it formed a major occupation period at the site. Stratigraphic levels dating with Late Classic materials may have been partially removed to create the reservoir itself. The perturbation is also reflected in the inversion of AMS radiocarbon dating with a Late Preclassic date at level 9 and a Late Classic to early Terminal Classic period date at level 10. A second line of evidence to that effect comes from the coarse fraction profile of this reservoir (Appendix C) which shows a marked contrast of levels 6 to 9 (coarse fraction at 18.9 % with SD of 3.4 (N = 4)) compared with levels both above (coarse fraction at 57.0 % with SD of 9.7 (N = 5)) and lower (coarse fraction of 54.6 % with SD of 7.6 (N = 6)) than this horizon. Terminal Classic ceramics were identified in levels 1–9, and an AMS date from level 3 corresponds to the Postclassic period. Like the other reservoirs, the heightened mercury concentrations were from the Terminal Classic context or later (levels1-7) with average mercury recorded as 3.17 µg g^{-1}, 270 % higher than the average mercury concentration prior to this period which is 1.18 µg g^{-1}.

4.4. Background samples

The 4 samples collected in Terminal Classic soils within the city core but outside the drainage basins of the reservoirs also showed high levels of mercury (Appendix C). The highest concentration with 6.44 µg $g^{-1}$of mercury (narrowly missing Benchmark 4) was from a ceremonial zone of the site (sample UCA20B-7-3-2074). It was excavated from plaza fill located directly in front of Stela 29 in sector H-10. Stela 29 was erected in the Terminal Classic period (Halperin and Martin 2020). The sample (UCA2F-19-3-2568) excavated at the edge of Ballcourt 1 in Plaza A was collected from a feasting midden context with large quantities of ceramics and contained 4.97 µg g^{-1} of mercury. Samples (JT004, JT005) located within the city, but away from public ceremonial zones presented somewhat lower concentrations of 3.02 and 3.78 µg g^{-1}. Finally, a sample (JT006) collected within the city, but in an area with no residential or ceremonial architecture, had a mercury concentration of 0.23 µg g^{-1}. At 3 times Benchmark 1, we consider this sample to be representative of what could be the lowest mercury concentrations likely to be found within the site core of Ucanal.

4.5. Soil conditions as indicators for mercury evasion

There is little doubt that some Hg^0 could have been lost during sediment deposition and diagenesis including drought events, as well as during sample collection and subsequent manipulations. Nonetheless, our analysis indicates that the soil at the site was not conducive to high mercury evasion. The pH measurements ranged from 7.3 to 7.9 throughout all samples (Appendix C), indicative of a slightly alkaline context at the site in general and a lower mercury evasion than what would be expected under acidic pH environments (Takeno 2005:115–117). As for the redox environment, the ancient water surface was an oxidizing environment while the accumulating sediments were likely reducing. Published data suggest that Hg^0 evasion fluxes from soils vary with organic content (Gustin and Stamenkovic 2005). Total organic carbon was measured in the reservoirs and was typically in the 1–2 % range except for the humic levels (top 30–40 cm) where it typically reached 4–8 %. A study by Poulin et al (2016) demonstrated distinct temporal differences in mercury transformation and release dynamics between soil horizons where mercury bound to organic matter dominated at high Eh (oxidation conditions) and at pH 7–8, while Hg^0 is to be expected at neutral to low Eh in lower horizons (in their case 20–30 cm). Considering the recorded pH and based on Eh(V)-pH

speciation profiles for mercury (Takeno 2005:115–117), a reducing environment of about −0.5 Eh(V) would have been required to generate Hg^0.

5. Discussion

Mercury concentrations above Benchmark 3 were identified in all three reservoir contexts and all non-reservoir background urban contexts at the site of Ucanal with the exception of a background (JT006) sample located away from residential and ceremonial architecture. Although we might expect to find higher concentrations of mercury in elite households or public ceremonial contexts due to the exotic and imported nature of cinnabar in Lowland Maya sites, both elite and non-elite urban residents of Ucanal either had access to mercury source materials or had the potential to be exposed to water with mercury mobilized through rain and erosion.

These findings are supported by some initial geochemical research in non-elite contexts elsewhere in Mesoamerica. For example, in a study at the village site of Cerén in El Salvador at the southernmost extent of the Classic Maya area, Parnell et al. (2002) recorded mercury concentrations between 3.58 and 10.14 μg g^{-1} from midden (at various depths), agricultural fields, and from a ceremonially important household, Structure 10, where the highest concentrations were found. The authors associate these mercury concentrations with the use of cinnabar pigments in these contexts and to the disposal of craft-related garbage.

Similarly, despite the ubiquity of mercury at the site of Ucanal, relatively higher concentrations may have corresponded, in part, to particular types of activities and deposition patterns. Among the non-reservoir samples, higher concentrations were found in ceremonial plaza spaces where ceremonial use of cinnabar may have occurred through caching of cinnabar, mercury, or cinnabar-decorated objects. Such concentrations may also be associated with middens in general. For example, some of the highest concentrations of mercury from P2C1 were also found in levels with high concentrations of domestic midden materials (levels 3–8) (Gauthier and Flynn-Arajdal 2024:148-149). Likewise, some of the highest concentrations recorded at Ucanal derived from the stratigraphic levels of Aguada 3 where high concentrations of trash had accumulated, particularly in levels 3–5 (Halperin et al. 2023b:134). Excavations of the two households surrounding the reservoir revealed evidence of Terminal Classic period artisanal activities in the form of bone tool and greenstone production debris, some of which were also found in levels 3–5 in the reservoir itself (Halperin et al. 2023b; Halperin et al. 2024a). A small paint pot lined with cinnabar-based pigment (UCA25B-3-4-3665) was also found in one of these households (Group 478). Thus, one possibility is that elevated concentrations of mercury derived from artisanal activities in the nearby households and/or materials accumulated as part of trash deposits. In addition, a human burial, Burial 23-1, was excavated from an adjacent excavation unit (2 m away from the sample collection zone) in Aguada 3. Although it was not a formal burial and did not possess grave furniture or grave goods, the arms and legs of the male individual (in his 50s) were tightly hugging the body, suggesting that he was bundled with cloth or matting before having been slid into the reservoir (Halperin et al. 2023:135, Fig.6.17). We cannot exclude the possibility that cinnabar could have been used as part of a ritual involving this burial, potentially increasing some of our mercury readings, even if no visible cinnabar was present upon excavations. Such funerary practices with cinnabar, however, are primarily recorded among royal tombs comprising the highest elite individuals of society (Fitzsimmons 2009:81–83) and not well-known among commoner populations. Nevertheless, the high concentrations of midden materials and the burial might suggest that Aguada 3 may have been an area to dispose of 'grey' or wastewater at some point during its life history.

The findings at Ucanal correspond to patterns found elsewhere in the Maya area in which the presence of mercury appears to be relatively widespread among ancient Maya sites but are found in particularly high concentrations in contexts related to artisanal activities, middens, or the locations of burials or offerings (Cook et al. 2006, 2022; Fulton et al. 2017; Hutson and Terry 2006). For example, Turner et al. (2021:880,890) found evidence of mercury in midden-rich and artefact-rich anthrosol at the Classic Maya site of Marco Gonzalez, Belize. They registered total mercury concentrations spanning from 0.05μg g^{-1} (background level) to a maximum of 1.33 μg g^{-1} adjacent to Structure 23 located at the center of the site. Their study found that mercury in surface soils was particularly linked to small surface depressions, use areas (structures) and vegetation (source of organic matter) as influencing factors on soil geochemistry. At the Late Classic site of Cancuén, Guatemala, a hot spot of 1 μg g^{-1} total mercury was recorded in soils at the southern edge of a burial that contained two ceramic offerings which may have contained cinnabar (Cook et al. 2006:634,636). This study also included measurements in domestic living spaces where mercury concentrations of up to 0.21 μg g^{-1} were detected; 5 times the local maximum pre-settlement mercury level estimated to be at 0.042 μg g^{-1}. Wells et al. (2000) recorded total mercury concentrations between 3 and 4 μg g^{-1} in sector U of Piedra Negras, Guatemala, with readings of 4.8 μg g^{-1} in midden deposits near a dedicatory cache containing ceramic vessels, one of which was dusted with cinnabar (Wells et al. 2000:457). High mercury concentrations were also found in soil collected near a wall (Hg at 5.6 μg g^{-1}), which the authors propose was once painted with cinnabar-based pigment, and in a royal domestic midden (Hg at 2.7 μg g^{-1}) containing a dense number of ceramics, that included decorated ceramics with hieroglyphic texts (Wells et al. 2000:455). These concentrations contrast with mercury levels considered to occur naturally, such as those recorded from a lake sediment profile with total mercury concentrations at 0.11 μg g^{-1} at Lake Petén Itza, Petén Guatemala, which may correlate with a known eruption of stratovolcano Acetanango in southern Guatemala at ca 2250 BP (Battistel et al. 2018).

Although few previous studies provide diachronic understandings of mercury compositions in soils, the results from both Lentz et al. (2020)'s study of reservoirs at Tikal and the Ucanal reservoir study reported here reveal significant increases in mercury at the end of the Classic period. The Tikal investigation recorded substantial increases at the very end of the Late Classic period with total mercury concentrations reaching 17 μg g^{-1} in dried sediments dating to the transition between the Late Classic and the Terminal Classic periods. This reading is in line with the maximum concentration of 16.91 μg g^{-1} detected in Terminal Classic dried sediments in Aguada 3 at Ucanal. All three reservoirs in Ucanal show a dramatic increase in total mercury contamination during the Terminal Classic period compared to earlier periods. This increase is evident in Aguada 2 with a 360 % increase compared to relatively stable mercury concentrations over a millennium before the Terminal Classic period. Aguada 3 shows an even more dramatic increase (at 3000 %), but this situation might be partially attributed to other factors, such as a burial or possible artisanal activities, as discussed earlier. Being a more dynamic environment with more rapid in and outflow of water, P2C1 did not accumulate mercury through the same processes than the Aguadas 2 and 3. Contaminated soils were deposited within it, however, and it shows a 270 % increase in the Terminal Classic compared to average mercury concentration recorded in levels associated with earlier periods.

At Ucanal, the increase in sedimentary mercury concentrations corresponded to a moment of political resurgence at the site. In addition, the Terminal Classic period was a moment of peak occupation at the site with 100 % of all tested residential groups occupied during this time (Halperin et al. 2021; Halperin and Ramos Hermandez 2024:Annex 2). At Tikal, however, increases in mercury contamination did not correlate with city growth and political power since Tikal experienced important moments of political consolidation and urban renewal during earlier periods, most notably during the Early Classic period after key moments of interaction with Teotihuacan and also during the beginning of the Late Classic period. In turn, both political influence and settlement population at the site diminished during the Terminal Classic period

(Sabloff 2003; Valdés and Fahsen 2004), when mercury levels were at their peak.

Another possibility for the increase in mercury levels at the two sites may be related to changing dynamics in trade relationships throughout various areas of the Maya Lowlands (Arnauld et al. 2017; Halperin et al. 2020; Sharer et al. 2006). During the 9th century, after the decline of power in large political centers in the Southern Lowlands, Ucanal expanded its political influence to become a small regional power with an increase in long-distance trade in ground stone from the Highlands and wider trade and alliance networks in general as understood from ceramics, iconography and marine shells found at the site. While the increase in mercury levels in the Terminal Classic might be linked to a more active trading network involving Ucanal, we cannot assume in all cases, such as at Tikal, a direct correlation between higher mercury levels and political-economy prosperity.

This research highlights the possibility that ancient Maya peoples were living in anthropogenically altered environments that could pose adverse health effects. Numerous epidemiological studies indicate that inorganic mercury salts are linked to cardiovascular, hematological, immunological and reproductive effects (ATSDR 2022) as the mechanisms of toxicity of mercury compounds are diverse and include targets that are common to all cells, such as mitochondrial function, neurotransmitter release and DNA methylation. More specifically, mercury exposure may lead to atherosclerosis, hypertension and insulin resistance (Tinkov et al. 2015). Exposure to mercury by Ucanal inhabitants could have come from several vectors of contamination such as water consumption, involuntary inhalation/ingestion while grinding or processing cinnabar or through directly handling cinnabar or other forms of mercury during rituals. The tolerable daily intake for inorganic mercury salts for oral ingestion exposure has recently been established at 2 μg kg^{-1} per day (ATSDR 2022).

Evidence of mercury exposure via inhalation or consumption of contaminated food or liquids in bone tissues from human remains is difficult to establish. A study from Cervini-Silva et al (2021), which discusses the chemical transformations of mercury leading to its incorporation into bone over millennia through various chemical processes involving $[(Hg_2)_3(PO_4)_2]$ and HgO (attributed to the presence of oxygen-containing ligands such as $P_2O_7^{4-}$), reveals the complexity of distinguishing between the accumulation of Hg into bone structures from environmental exposure over a life time and the detection of Hg in bone remains exposed to cinnabar through funerary practices. Mercury, however, can concentrate at interstitial positions of the bone matrix, can be found within the interior pores of bones (Cervini-Silva et al. 2021), or can be distributed in bone hydroxyapatite (Ávila et al. 2014). These recent findings will guide future research from the perspective of human remains at Ucanal.

6. Conclusion

Mercury contamination, likely through the direct use of cinnabar and its mobilization through soil and water, was pervasive at the ancient Maya city of Ucanal. Residents of the city appear to have been exposed to anthropogenic-derived mercury from at least the Late Preclassic to the Terminal Classic periods. All 3 tested reservoirs, however, show a dramatic increase in total mercury contamination during the Terminal Classic period compared to readings from earlier periods. These increases are consistent between the reservoirs despite different water catchment zones, social status associations, and hydrological capabilities of the reservoirs. Aguada 2 had the largest diachronic depth from at least the Late Preclassic to the Terminal Classic periods and encompassed a drainage area that included elite residences. Aguada 3′s mercury contamination potentially came from artisanal or funerary activities associated with the low and middle-status residences surrounding it. Piscina 2 of Canal 1 was immediately surrounded by commoner residences but had the largest drainage area encompassing ceremonial plaza spaces and both elite and commoner residences. Although Piscina 2 was a dynamic rather than stagnant reservoir, mercury accumulations also increased during the Terminal Classic period. These findings suggest a possible exacerbation of the mercury related exposure for city residents during this time, a subject of research that needs to be explored further from the perspective of human remains at the site and elsewhere in the Maya area.

CRediT authorship contribution statement

Jean D. Tremblay: Writing – original draft, Methodology, Investigation, Formal analysis, Data curation. **Christina T. Halperin:** Writing – review & editing, Validation, Supervision, Project administration, Investigation, Funding acquisition, Conceptualization. **Peter M.J. Douglas:** Writing – review & editing, Validation, Supervision, Methodology, Investigation.

Declaration of competing interest

The authors declare that they have no known competing financial interests or personal relationships that could have appeared to influence the work reported in this paper.

Data availability

Data will be made available on request.

Acknowledgements

Funding for research derived from a Canadian Social Sciences and Humanities Research Council Insight Grant (no. 435-2021-0462) and a Direction des Affaires Internationales travel grant from the Université de Montréal. Research by the PAU would not be possible without the support and participation of the community of Pichelito located on and by the site of Ucanal, our colleagues from Barrio Nuevo San José and project laboratory staff headed by Miriam Salas Pol (https://www.ucanal-archaeology.com). We are also grateful to the Departmento de Monumentos Prehistoricos y Coloniales from the Ministerio de Culture y Deportes in Guatemala for their support and permission to work at Ucanal. Finally, we wish to express our gratitude to Laurianne Gauthier and Yasmine Flynn- Ajajdal for the excavation of Piscina 2 of Canal 1, and to Carlos Gomez-Cruz for the excavation of Aguada 2.

Appendix A

Age/depth profile: Aguadas 2, 3 and P2C1 AMS radiocarbon dating and ceramic chronologies. Ceramic chronologies established by PAU.

Table A.1
Aguada 3, AMS radiocarbon dating and ceramic (PAU) chronologies.

Depth (cm)	AMS Radiocarbon dating	Ceramic phases
10		Terminal Classic (late phase)
20		Terminal Classic (late phase)
30	774–777 CE 1.3 %; 783–881 CE 94.2 %	Terminal Classic (late phase)
40		Terminal Classic (late phase)
50		Terminal Classic (early phase), mixed
60		Terminal Classic
70		Late Classic, mixed
80		Late Classic, mixed with some Late Preclassic sherds
90		Late Classic, mixed with some Late Preclassic sherds
100		Late Classic, mixed with some Late Preclassic sherds
110	660–706 CE 46.7 %; 737–775 CE 48.7 %	Late Classic mixed with some Late Preclassic sherds
120		Middle Preclassic

Table A.2
P2C1, AMS radiocarbon dating and ceramic (PAU) chronologies.

Depth (cm)	AMS Radiocarbon dating	Ceramic phases
10		Terminal Classic (late phase)
20		Terminal Classic (late phase)
30	1302–1368 CE 75.0 %; 1381–1398 CE 20.4 %	Terminal Classic (late phase)
40		Terminal Classic (late phase)
50		Terminal Classic (early phase)
60		Terminal Classic
70		Terminal Classic
80		Terminal Classic (early phase)
90	365–341 BCE 13.3 %; 323–200 BCE 82,.%	Terminal Classic (with small quantities of Late Preclassic sherds)
100	690–695 CE 1.0 %; 701-741AD 32.7 %; 771–779 CE 3.3 %; 786–835 CE 50.4 %; 850–876 CE 8.1 %	Mixed Late Classic, Early Classic, and Late Preclassic sherds
110		Terminal Preclassic, mixed with some Early Classic sherds
120		Mixed Late Classic, Early Classic, and Late Preclassic sherds
130		Late Preclassic mixed with small quantities of Early Classic period sherds
140	352–287 BCE 47.9 %; 228–218 BCE 1.5 %; 211–155 BCE 46.0 %	Late Preclassic mixed with small quantities of Classic period sherds
150		Early Classic, mixed with 1 Late Classic sherd

Table A.3
Aguada 2, AMS radiocarbon dating and ceramic (PAU) chronologies.

Depth (cm)	AMS Radiocarbon dating	Ceramic phases
10		Terminal Classic, (late phase)
20		Terminal Classic (late phase)
30		Terminal Classic (late phase)
40		Terminal Classic (early phase), mixed
50	665–709 CE 42.9 %; 723–775 CE 52.5 %	Terminal Classic (early phase), mixed
60		Late Classic (B'aaluum), mixed
70		Late Classic (B'aaluum)
80		Late Classic (B'aaluum)
90		Late Classic (Kan), mixed
100		Late Classic (Kan), mixed
110		Late Classic (Kan), mixed
120		Late Classic (Kan), mixed
130		Late Classic (Kan), mixed
140		Early Classic, mixed
150	422–539 CE 95.4 %	Early Classic, mixed
160		Early Classic, mixed
170		Early Classic, mixed
180		Early Classic, small amounts of Late Preclassic
190		Early Classic and Late Preclassic mixed
200		Early Classic and Late Preclassic mixed
210		Early Classic and Late Preclassic mixed
220	72–210 CE 95.4 %	Early Classic and Late Preclassic mixed
230		Terminal Preclassic
240		Terminal Preclassic

(*continued on next page*)

Table A.3 (*continued*)

Depth (cm)	AMS Radiocarbon dating	Ceramic phases
250		Terminal Preclassic
260		Late Preclassic
270		Late Preclassic
280		Middle Preclassic (‘Ayin)
290		Middle Preclassic (‘Ayin)
300	165–47 BC 95.4 %	Middle Preclassic (‘Ayin)
310		Middle Preclassic (‘Ayin and pre-‘Ayin), mixed
320		Middle Preclassic (‘Ayin and pre-‘Ayin), mixed
330		Middle Preclassic (‘Ayin and pre-‘Ayin), mixed
340	355–281 BCE 52.5 %; 231–157 BCE 43.0 %	Middle Preclassic (pre-‘Ayin), mixed
350		Middle Preclassic (‘Ayin and pre-‘Ayin)

Table A.4
Complementary tracking radiocarbon information for Aguada 2, 3 and P2C1: University of Ottawa Lab sample ID, location & depth, material tested, and ^{14}C yr BP.

Lab ID tracking	Location & depth	Material	^{14}C yr. BP (non-calibrated)
UOC-23721	Aguada 3, 30 cm	Charcoal	1220 ± 20
UOC-20025	Aguada 3, 110 cm	Charcoal	1309 ± 18
UOC-20026	Aguada 2, 50 cm	Charcoal	1295 ± 18
UOC-20027	Aguada 2, 150 cm	Charcoal	1599 ± 18
UOC-20029	Aguada 2, 220 cm	Charcoal	1903 ± 18
UOC-23722	Aguada 2, 300 cm	Charcoal	2100 ± 20
UOC-20028	Aguada 2, 340 cm	Clay like sediments mixed with charcoal	2172 ± 19
UOC-23717	Piscina 2, 30 cm	Charcoal	615 ± 20
UOC-23719	Piscina 2, 90 cm	Charcoal	2220 ± 20
UOC-23718	Piscina 2, 100 cm	Charcoal	1240 ± 20
UOC-23720	Piscina 2, 140 cm	Charcoal	2170 ± 20

Appendix B

QA/QC data from Aguadas 2 and 3 and P2C1. Randomly selected samples were run as triplicates and submitted to parallel laboratory preparation and analyses. We report here on two conservative global error calculations.

Table B.1
QA/QC samples locations, depth, and mercury concentrations of Ucanal reservoirs.

Location	Depth (cm)	Triplicates	Hg (μg/g)
Aguada 2	50	Ta	1.06
Aguada 2	50	Tb	1.08
Aguada 2	50	Tc	1.93
Aguada 2	140	Ta	0.53
Aguada 2	140	Tb	0.58
Aguada 2	140	Tc	0.49
Aguada 2	220	Ta	0.58
Aguada 2	220	Tb	0.59
Aguada 2	220	Tc	0.92
Aguada 2	300	Ta	0.92
Aguada 2	300	Tb	0.87
Aguada 2	300	Tc	0.65
Aguada 3	30	Ta	15.98
Aguada 3	30	Tb	15.10
Aguada 3	30	Tc	19.64
Aguada 3	80	Ta	0.16
Aguada 3	80	Tb	0.18
Aguada 3	80	Tc	0.13
Piscina 2	60	Ta	3.13
Piscina 2	60	Tb	3.29
Piscina 2	60	Tc	3.39
Piscina 2	140	Ta	0.87
Piscina 2	140	Tb	1.23
Piscina 2	140	Tc	1.04

Table B.2
Global error of 14.5 % Calculations based on the mean of variation coefficients.

Location	Ta (μg/g)	Tb (μg/g)	Tc (μg/g)	Mean (μg/g)	SD (μg/g)	VC
Aguada 3, 30 cm	15.98	15.10	19.64	16.907	1.966	0.116
Aguada 3, 80 cm	0.16	0.18	0.13	0.157	0.021	0.131
Aguada 2, 50 cm	1.06	1.08	1..93	1.357	0.405	0.299
Aguada 2, 140 cm	0.53	0.58	0.49	0.533	0.037	0.069
Aguada 2, 220 cm	0.58	0.59	0.92	0.697	0.158	0.227
Aguada 2, 300 cm	0.92	0.87	0.65	0.813	0.117	0.144
Piscina 2, 60 cm	3.13	3.29	3.39	3.270	0.107	0.033
Piscina 2, 140 cm	0.87	1.23	1.04	1.047	0.147	0.140

Table B.3
Global error of 14.3 %) Calculations based on the mean standard deviation of our QA/QC samples (0.370 μg g^{-1}) divided by the mean of data set concentrations (2.59μg g^{-1}).

Location	Ta (μg/g)	Tb (μg/g)	Tc (μg/g)	Mean (μg/g)	SD ((μg/g))
Aguada 3, 30 cm	15.98	15.10	19.64	16.907	1.966
Aguada 3, 80 cm	0.16	0.18	0.13	0.157	0.021
Aguada 2, 50 cm	1.06	1.,08	1.93	1.357	0.405
Aguada 2, 140 cm	0.53	0.58	0.49	0.533	0.037
Aguada 2, 220 cm	0.58	0.59	0.92	0.697	0.158
Aguada 2, 300 cm	0.92	0.87	0.65	0.813	0.117
Piscina 2, 60 cm	3.13	3.29	3.39	3.270	0.107
Piscina 2, 140 cm	0.87	1.23	1.04	1.047	0.147

Appendix C

Mercury concentrations with depth for Aguadas 2 and 3, P2C1, and background samples collected throughout Ucanal city core. Coarse fraction profile for P2C1 and soil pH measurements.

Table C1
Aguada 2 mercury concentrations with depth. (for QA/QC samples, average of the triplicates is used).

Depth (cm)	Hg (μg/g)
10	3.80
20	4.45
30	3.99
40	1.81
50	1.36
60	0.87
70	0.81
80	0.70
90	0.77
100	0.84
110	0.55
120	0.53
130	0.49
140	0.53
150	0.68
160	1.12
170	1.55
180	0.95
190	0.64
200	1.32
210	0.56
220	0.70
230	0.48
240	0.69
250	1.21
260	0.83
270	0.62
280	0.72
290	0.72
300	0.81
310	0.92
320	1.37
330	1.21
340	1.35
350	0.73

Table C.2
Aguada 3 mercury concentrations with depth. (for QA/QC samples, average of the triplicates is used).

Depth	Hg (μg/g)
10	14.25
20	15.07
30	16.91
40	13.19
50	6.76
60	2.36
70	1.07
80	0.16
90	0.01
100	0.54
110	0.20
120	0.16

Table C.3
P2C1 mercury concentrations with depth. (for QA/QC samples, average of the triplicates is used).

Depth	Hg (μg/g)
10	3.11
20	2.93
30	3.69
40	3.34
50	3.06
60	3.13
70	4.12
80	1.97
90	2.00
100	1.54
110	0.96
120	1.04
130	0.82
140	0.87
150	1.03

Table C.4
Background mercury samples from within Ucanal city core. For sample locations please refer to Fig. 2.

Sample ID	Hg (μg/g)	Period	Context
JT004	3.02	10 cm from ground surface,Terminal Classic	Small depression near Group 785
JT005	3.78	10 cm from ground surface,Terminal Classic	Residential Group 575
JT006	0.23	10 cm from ground surface,Terminal Classic	Clearing zone away from architecture
UCA20B-7-3-2074	6.44	Plaza fillLate Terminal Classic	Plaza area in font of Stela 29, Plaza K
UCA2F-19-3-2568	4.97	Midden,Terminal Classic	Ballcourt 1, Plaza A

Table C.5
P2C1 coarse fraction with depth.

Depth (cm)	Coarse portion % > 2.36 mm
10	65.1
20	65.9
30	49.9
40	43.9
50	60.4
60	20.9
70	13.9
80	19.6
90	21.2
100	57.1

(*continued on next page*)

Table C.5 (*continued*)

Depth (cm)	Coarse portion % > 2.36 mm
110	56.4
120	49.7
130	67.8
140	48.2
150	48.1

Table C.6
Soil pH values from reservoirs and surrounding environments.

Location & depth	pH
Aguada 3, 30 cm	7.28
Aguada 3, 80 cm	7.87
Aguada 2, 50 cm	7.61
Aguada 2, 140 cm	7.51
Aguada 2, 220 cm	7.65
Aguada 2, 300 cm	7.56
Piscina 2 of Canal 1, 60 cm	7.43
Piscina 2 of Canal 1, 140 cm	7.45
JT006, 10 cm	7.32

References

Arnauld, Marie Charlotte, Chloé Andrieu, and Mélanie Forné 2017. In the days of my life." Elite activity and interactions in the Maya lowlands from Classic to Early Postclassic times (the long ninth century, AD 760-920). Journal de la Société des américanistes(Maya times). DOI:10.4000/jsa.15362, accessed February 24, 2024.

ATSDR, 2022. Toxicological Profile for Mercury. U.S. Department of Health and Human Services. Https://www.atsdr.cdc.gov/toxprofiles/tp46.pdf.

Ávila, A., Mansilla, J., Bosch, P., Pijoan, C., 2014. Cinnabar in Mesoamerica: poisoning or mortuary ritual? J. Archaeol. Sci. 49, 48–56. https://doi.org/10.1016/j.jas.2014.04.024.

Bank, Michael S., 2012. Mercury in the Environment: Pattern and Process. 1 online resource (361 pages) vols. University of California Press, Berkeley.

Battistel, D., Roman, M., Marchetti, A., Kehrwald, N.M., Radaelli, M., Balliana, E., Toscano, G., Barbante, C., 2018. Anthropogenic impact in the Maya Lowlands of Petén, Guatemala, during the last 5500 years. J. Quat. Sci. 33 (2), 166–176. https://doi.org/10.1002/jqs.3013.

Canada Environment and Climate Change Canada, 2016. Canadian mercury science assessment: report. 1 online resource (793 pages) vols. Environment and Climate Change Canada = Environnement et changement climatique Canada, Gatineau, QC.

Canuto, M.A., Estrada-Belli, F., Garrison, T.G., Houston, S.D., Acuña, M.J., Kováč, M., Marken, D., Nondédéo, P., Auld-Thomas, L., Castanet, C., Chatelain, D., Chiriboga, C. R., Drápela, T., Lieskovský, T., Tokovinine, A., Velasquez, A., Fernández-Díaz, J.C., Shrestha, R., 2018. Ancient lowland Maya complexity as revealed by airborne laser scanning of northern Guatemala. Science 361. https://doi.org/10.1126/science.aau0137.

CCME 2007 *Canadian Soil Quality Guidelines for the Protection of Environmental and Human Health*. https://support.esdat.net/Environmental%20Standards/canada/soil/rev_soil_summary_tbl_7.0_e.pdf.

Cervini-Silva, J., Palacios, E., De Lourdes, M., Muñoz, P.D., Angel, J.A., Montoya, E.R., López, F., Pacheco, A.R., 2013. Cinnabar-preserved bone structures from primary osteogenesis and fungal signatures in ancient human remains. Geomicrobiol J. 30 (7), 566–577. https://doi.org/10.1080/01490451.2012.737090.

Cervini-Silva, J., de Lourdes, M., Muñoz, E.P., Jimenez-Lopez, J.C., Romano-Pacheco, A., 2018. Ageing and preservation of HgS-enriched ancient human remains deposited in confinement. J. Archaeol. Sci. Rep. 18, 562–567. https://doi.org/10.1016/j.jasrep.2018.02.010.

Cervini-Silva, J., de Lourdes, M., Muñoz, E.P., Ufer, K., Kaufhold, S., 2021. Natural incorporation of mercury in bone. Journal of Trace Elements in Medicine and Biology 67, 126797. https://doi.org/10.1016/j.jtemb.2021.126797.

Christopherson, R.W., 2009. Geosystems: an introduction to physical geography, Seventh edition. Pearson, NY, NY.

Coe, Michael Douglas, Houston, Stephen D., 2015. The Maya. Ninth ed. Ancient peoples and places. Thames & Hudson, London.

Cook, D.E., Kovacevich, B., Beach, T., Bishop, R., 2006. Deciphering the inorganic chemical record of ancient human activity using ICP-MS: a reconnaissance study of late Classic soil floors at Cancuén, Guatemala. J. Archaeol. Sci. 33 (5), 628–640. https://doi.org/10.1016/j.jas.2005.09.019.

Cook, D.E., Beach, T.P., Luzzadder-Beach, S., Dunning, N.P., Turner, S.D., 2022. Environmental legacy of pre-Columbian Maya mercury. Front. Environ. Sci. 10, 2023. https://doi.org/10.3389/fenvs.2022.986119, accessed April 18.

Couoh, L.R., 2015. Bioarchaeological Analysis of a Royal Burial from the Oldest Maya Tomb in Palenque, Mexico. Int. J. Osteoarchaeol. 25 (5), 711–721. https://doi.org/10.1002/oa.2338.

Crann, Carley A, Sarah Murseli, Gilles St-Jean, Xiaolei Zhao, Ian D Clark, William E Kieser, 2017. First Status Report on Radiocarbon Sample Preparation Techniques at the A.E. Lalonde AMS Laboratory (Ottawa, Canada). Radiocarbon 59(3):695–704. DOI:10.1017/RDC.2016.55.

Dill, H.G., 2010. The "chessboard" classification scheme of mineral deposits: Mineralogy and geology from aluminum to zirconium. Earth Sci. Rev. 100 (1), 1–420. https://doi.org/10.1016/j.earscirev.2009.10.011.

Dunning, N., Beach, T., Farrell, P., Luzzadder-Beach, S., 1998. Prehispanic agrosystems and adaptive regions in the maya lowlands. Culture Agriculture 20 (2–3), 87–101. https://doi.org/10.1525/cag.1998.20.2-3.87.

Dunning, N., Scarborough, V., Valdez, F., Luzzadder-Beach, S., Beach, T., Jones, J.G., 1999. Temple mountains, sacred lakes, and fertile fields: ancient Maya landscapes in northwestern Belize. Antiquity 73 (281), 650–660. https://doi.org/10.1017/S0003598X0006525X.

Environment Canada 2010. Risk Management Strategy for Mercury. https://www.ec.gc.ca/doc/mercure-mercury/1241/index_e.htm#gotoC00.

Espíndola, J.M., Macías, J.L., Tilling, R.I., Sheridan, M.F., 2000. Volcanic history of El Chichón Volcano (Chiapas, Mexico) during the Holocene, and its impact on human activity. Bull. Volcanol. 62 (2), 90–104. https://doi.org/10.1007/s004459900064.

Ferrara, R., Ceccarini, C., Lanzillotta, E., Gårdfeldt, K., Sommar, J., Horvat, M., Logar, M., Fajon, V., Kotnik, J., 2003. Profiles of dissolved gaseous mercury concentration in the Mediterranean seawater. Atmos. Environ. 37. Dynamic processes of mercury and other trace contaminants in the marine boundary layer of european seas - ELOISE II:85–92. DOI:10.1016/S1352-2310(03)00248-6.

Fitzsimmons, James L., 2009 Death and the classic Maya kings. The Linda Schele series in Maya and pre-columbian studies. University of Texas Press, Austin.

Folan, W.J., 1983. Physical Geography of the Yucatan Peninsula. In: Coba. Elsevier, pp. 21–48.

Fulton, Kara A., Christian Wells, E., Storer, Donald A., 2017. Ritual or residential? An integrated approach to geochemical prospection for understanding the use of plaza spaces at Palmarejo, Honduras. Archaeol. Anthropol. Sci. 9(6), 1059–1076. DOI: 10.1007/s12520-013-0170-3.

Gallagher, David, Perez Siliceo, Rafael, 1948. Geology of the huahuaxtla mercury district state of guerrero, MEXICO. UNITED STATES DEPARTMENT OF THE INTERIOR, Washington.

Gaudet, C., Lingard, S., Cureton, P., Keenleyside, K., Smith, S., Raju, G., 1995. Canadian environmental quality guidelines for mercury. Water Air Soil Pollut. 80 (1), 1149–1159. https://doi.org/10.1007/BF01189777.

Gauthier, Laurianne, Flynn-Arajdal, Yasmine, 2024. Excavaciones En La Piscina 2 Del Canal 1 Del Sitio Arqueológico Ucanal: Operación 29A. In: Proyecto Arqueolóco Ucanal, 7a Temporada de Campo 2023. Edited by Christina T. Halperin and Carmen Ramos Hermandez., pp. 146–164. Report submitted to the Dirección General del Patrimonio Cultural y Natural, Guatemala., Guatemala.

Gifford, James C., 1976. Prehistoric pottery analysis and the ceramics of Barton Ramie in the Belize Valley. Memoirs of the Peabody Museum of Archaeology and Ethnology, Harvard University v. 18. Peabody Museum of Archaeology and Ethnology, Harvard University, Cambridge, Mass.

Cruz Gómez, Carlos, Quezada, Mario, 2023. Excavaciones En El Grupo de La Aguada #2 Del Sitio Arqueolóico Ucanal (Operación 22). In Proyecto Arqueológico Ucanal: 6ta Temporada de Campo, 2022. Christina T. Halperin and Jose Luis Garrido López, eds.

Report submitted to the Dirección General del Patrimonio Cultural y Natural, Guatemala., Guatemala.
Gonzalez-Raymat, H., Liu, G., Liriano, C., Li, Y., Yin, Y., Shi, J., Jiang, G., Cai, Y., 2017. Elemental mercury: Its unique properties affect its behavior and fate in the environment. Environ. Pollut. 229, 69–86. https://doi.org/10.1016/j.envpol.2017.04.101.
Gorokhovich, Y., Block, K.A., McNeil, C.L., Barrios, E., Marionkova, M., 2020. Mercury source in Copan (Honduras): Local mining or trade? J. Archaeol. Sci. Rep. 33, 102471. https://doi.org/10.1016/j.jasrep.2020.102471.
Gunn, J.D., Matheny, R.T., Folan, W.J., 2002. Climate-change studies in the Maya area: a diachronic analysis. Anc. Mesoam. 13 (1), 79–84. https://doi.org/10.1017/S0956536102131105.
Gustin, M.S., Stamenkovic, J., 2005. Effect of Watering and Soil Moisture on Mercury Emissions from Soils. Biogeochemistry 76 (2), 215–232.
Halperin, Christina T., Yasmine Flynn-Arajdal, Katherine A. Miller Wolf, Carolyn Freiwald, 2021. Terminal Classic residential histories, migration, and foreigners at the Maya site of Ucanal, Petén, Guatemala. J. Anthropol. Archaeol. 64:101337. DOI: 10.1016/j.jaa.2021.101337.
Halperin, Christina T., Jose Luis Garrido (editors), 2023. Proyecto Arqueologico Ucanal: Septima Temporada de Campo Ano 2022. Report submitted to the Direction General Del Patrimonio Cultural y Natural, Guatemala.
Halperin, Christina T., Yasmine Flynn-Arajdal, Cynthia Bello-Hernandez, Noémie Bolduc, Laurianne Gauthier, Alex Mercier, and David Olivier 2023 Excavaciones En El Grupo 151 del Sitio Arqueológico Ucanal: (Operaciones 23A, 23B, 23C). In *Proyecto Arqueológico Ucanal: 6ta Temporada de Campo, 2022, edited by Christina T. Halperin and Jose Luis Garrido López*, pp. 125–154. Report submitted to the Direccion General del Patrimonio Cultural y Natural. Nueva Guatemala de la Asuncion. Guatemala.
Halperin, Christina T., Ramos Hermandez, Carmen E. 2024. Proyecto Arqueológico Ucanal: Informe Final. Septa Temporada de Campo 2023. Report submitted to the Dirección General del Patrimonio Cultural y Natural, Guatemala., Guatemala.
Halperin, Christina T., Liane Chalifour, Jonathan Crosato, Daphnée Hounzell, and Gabrielle Proux 2024. Excavaciones En El Grupo 478 Del Sitio Arqueológico Ucanal (Operaciones 25A, 25B, 25C). In Proyecto Arqueológico Ucanal, 7a Temporada de Campo, 2023. Christina T. Halperin and Carmen E. Ramos Hernandez, eds. Report submitted to the Ministerio de Cultura y Deportes, Dirección General del Patrimonio Cultural y Natural., Guatemala.
Halperin, Christina T., Jose Luis Garrido, Jean-Baptiste Le Moine, Miguel Angel Cano, Carlos Gomez-Cruz, Marta Perea, Yasmine Flynn-Arjadal, Maria Fernanda Lopez, and Katherine Miller-Wolf 2024 Coyunturas y continuidades en la larga historia de la antigua ciudad de Ucanal: Una mirada desde sus sistemas de manejo de agua, residencias y arquitectura ceremonial. In: XXXVI Simposio de Investigaciones Arqueológicas en Guatemala, edited by B. Arroyo and L. Paiz Aragon, Museo Nacional de Arqueología y Etnología de Guatemala, Guatemala.
Halperin, C.T., Garrido, J.L., 2020. Architectural Aesthetics, Orientations, and Reuse at the Terminal Classic Maya Site of Ucanal, Petén, Guatemala. J. Field Archaeol. 45 (1), 46–66. https://doi.org/10.1080/00934690.2019.1676033.
Halperin, C.T., Le Moine, J.-B., Zambrano, E.P., 2019. Infrastructures of moving water at the Maya site of Ucanal, Petén, Guatemala. J. Anthropol. Archaeol. 56, 101102. https://doi.org/10.1016/j.jaa.2019.101102.
Halperin, C.T., Lopez, J.L.G., Salas, M., LeMoine, J.-B., 2020. Convergence Zone Politics at the Archaeological Site of Ucanal, Petén, Guatemala. Ancient Mesoamerica 31 (3), 476–493. https://doi.org/10.1017/S0956536120000085.
Halperin, C.T., Martin, S., 2020. Ucanal stela 29 and the cosmopolitanism of terminal classic maya stone monuments. Lat. Am. Antiq. 31 (4), 817–837. https://doi.org/10.1017/laq.2020.70.
Hauser-Davis, Rachel Ann, Natalia Soares Quinete, Lemos, Leila Soledade (editors), 2023. Lead, Mercury and Cadmium in the Aquatic Environment: Worldwide Occurrence, Fate and Toxicity. CRC Press, Boca Raton.
Houston, Stephen D., 2009. Veiled brightness: a history of ancient Maya color. 1st ed. The William & Bettye Nowlin series in art, history, and culture of the western hemisphere. University of Texas Press, Austin.
Hutson, S.R., Terry, R.E., 2006. Recovering social and cultural dynamics from plaster floors: chemical analyses at ancient Chunchucmil, Yucatan Mexico. J. Archaeol. Sci. 33 (3), 391–404. https://doi.org/10.1016/j.jas.2005.08.004.
Keenan, B., Imfeld, A., Johnston, K., Breckenridge, A., Gélinas, Y., Douglas, P.M.J., 2021. Molecular evidence for human population change associated with climate events in the Maya lowlands. Quat. Sci. Rev. 258, 106904. https://doi.org/10.1016/j.quascirev.2021.106904.
Keenan, B., Imfeld, A., Gélinas, Y., Douglas, P.M.J., 2022. Understanding controls on stanols in lake sediments as proxies for palaeopopulations in Mesoamerica. J. Paleolimnol. 67 (4), 375–390. https://doi.org/10.1007/s10933-022-00238-9.
Kocman, D., Kanduč, T., Ogrinc, N., Horvat, M., 2011. Distribution and partitioning of mercury in a river catchment impacted by former mercury mining activity. Biogeochemistry 104 (1–3), 183–201. https://doi.org/10.1007/s10533-010-9495-5.
Köster, D., Pienitz, R., Wolfe, B., Barry, S., Foster, D., Dixit, S., 2005. Paleolimnological assessment of human-induced impacts on Walden Pond (Massachusetts, USA) using diatoms and stable isotopes. Aquat. Ecosyst. Health Manag. 8 (2), 117–131.
Kotra, J.P., Finnegan, D.L., Zoller, W.H., Hart, M.A., Moyers, J.L., 1983. El Chichón: composition of plume gases and particles. Science 222 (4627), 1018–1021.
Kulikova, T., Hiller, E., Jurkovič, Ľ., Filová, L., Šottník, P., Lacina, P., 2019. Total mercury, chromium, nickel and other trace chemical element contents in soils at an old cinnabar mine site (Merník, Slovakia): anthropogenic versus natural sources of soil contamination. Environ. Monit. Assess. 191 (5), 263. https://doi.org/10.1007/s10661-019-7391-6.
Kushner, D.S., Lopez, T.M., Wallace, K.L., Damby, D.E., Kern, C., Cameron, C.E., 2023. Estimates of volcanic mercury emissions from Redoubt Volcano, Augustine Volcano, and Mount Spurr eruption ash. Front. Earth Sci. 11, 2024. https://doi.org/10.3389/feart.2023.1054521, accessed July 3.
Laporte, Juan Pedro, Mejía, Héctor E., 2002. Ucanal: una ciudad del Río Mopan en Petén, Guatemala. U tz'ib. Serie reportes v. 1, no. 2. Asociación Tikal, Guatemala.
Laporte, Juan Pedro, 2007. La Secuencia Cerámica del Sureste de Petén: Tipos, Cifras, Localidades, y la Historia del Asentamiento. Dirección General del Patrimonio Cultural y Natural, Ministerio de Cultura y Deportes, Guatemala City., Guatemala City.
Lentz, D.L., Hamilton, T.L., Dunning, N.P., Scarborough, V.L., Luxton, T.P., Vonderheide, A., Tepe, E.J., Perfetta, C.J., Brunemann, J., Grazioso, L., Valdez, F., Tankersley, K.B., Weiss, A.A., 2020. Molecular genetic and geochemical assays reveal severe contamination of drinking water reservoirs at the ancient Maya city of Tikal. Sci. Rep. 10 (1), 10316. https://doi.org/10.1038/s41598-020-67044-z.
Liu, Guangliang, Yong Cai, O'Driscoll, Nelson J., 2012. Environmental chemistry and toxicology of mercury. 1 online resource (xix, 574 pages) : illustrations vols. Wiley, Hoboken, N.J.
Lucero, L.J., 2002. The collapse of the classic maya: a case for the role of water control. Am. Anthropol. 104 (3), 814–826. https://doi.org/10.1525/aa.2002.104.3.814.
Lucero, L.J., Gunn, J.D., Scarborough, V.L., 2011. Climate change and classic maya water management. Water 3 (2), 479–494. https://doi.org/10.3390/w3020479.
MacDonald, D.D., Ingersoll, C.G., Berger, T.A., 2000. Development and evaluation of consensus-based sediment quality guidelines for freshwater ecosystems. Arch. Environ. Contam. Toxicol. 39 (1), 20–31. https://doi.org/10.1007/s002440010075.
Martin, Simon, 2020. Ancient Maya politics: a political anthropology of the classic period, 150-900 CE. 1 online resource (xxi, 520 pages): illustrations, maps vols. Cambridge University Press, Cambridge, United Kingdom .
Martínez-Trinidad, S., Silva, G.H., Reyes, J.M., Munguía, G.S., Valdez, S.S., Islas, M.E.R., Martínez, R.G., 2013. Total mercury in terrestrial systems (air-soil-plant-water) at the mining region of San Joaquín, Queretaro, Mexico. *Geofísica Internacional* 52 (1), 43–58. https://doi.org/10.1016/S0016-7169(13)71461-2.
Millard, A.R., 2014. Conventions for reporting radiocarbon determinations. Radiocarbon 56 (2), 555–559. https://doi.org/10.2458/56.17455.
Miller, M.E., 2019. The art of Mesoamerica: from Olmec to Aztec, Sixth edition. World of art. Thames & Hudson, New York, New York.
Miller, M.E., Taube, K., 1993. The gods and symbols of ancient Mexico and the Maya: an illustrated dictionary of Mesoamerican religion. Thames and Hudson, London.
Murseli, S., Middlestead, P., St-Jean, G., Zhao, X., Jean, C., Crann, C.A., Kieser, W.E., Clark, I.D., 2019. The preparation of water (DIC, DOC) and Gas (CO 2, CH 4) samples for radiocarbon analysis at AEL-AMS, Ottawa, Canada. Radiocarbon 61 (5), 1563–1571. https://doi.org/10.1017/RDC.2019.14.
Némery, J., Gratiot, N., Doan, P.T.K., Duvert, C., Alvarado-Villanueva, R., Duwig, C., 2016. Carbon, nitrogen, phosphorus, and sediment sources and retention in a small eutrophic tropical reservoir. Aquat. Sci. 78 (1), 171–189. https://doi.org/10.1007/s00027-015-0416-5.
Noh, S., Kim, J., Hur, J., Hong, Y., Han, S., 2018. Potential contributions of dissolved organic matter to monomethylmercury distributions in temperate reservoirs as revealed by fluorescence spectroscopy. Environ. Sci. Pollut. Res. 25 (7), 6474–6486. https://doi.org/10.1007/s11356-017-0913-2.
Parnell, J.J., Terry, R.E., Nelson, Z., 2002. Soil chemical analysis applied as an interpretive tool for ancient human activities in Piedras Negras Guatemala. J. Archaeol. Sci. 29 (4), 379–404. https://doi.org/10.1006/jasc.2002.0735.
Pendergast, D.M., 1982. Ancient Maya Mercury. Science 217 (4559), 533–535. https://doi.org/10.1126/science.217.4559.533.
Polissar, P.J., D'Andrea, W.J., 2014. Uncertainty in paleohydrologic reconstructions from molecular δ*D* values. Geochim. Cosmochim. Acta 129, 146–156. https://doi.org/10.1016/j.gca.2013.12.021.
Poulin, B.A., Aiken, G.R., Nagy, K.L., Manceau, A., Krabbenhoft, D.P., Ryan, J.N., 2016. Mercury transformation and release differs with depth and time in a contaminated riparian soil during simulated flooding. Geochim. Cosmochim. Acta 176, 118–138. https://doi.org/10.1016/j.gca.2015.12.024.
Quintana, P., Tiesler, V., Conde, M., Trejo-tzab, R., Bolio, C., Alvarado-gil, J.J., Aguilar, D., 2015. Spectrochemical characterization of red pigments used in classic period maya funerary practices. Archaeometry 57 (6), 1045–1059. https://doi.org/10.1111/arcm.12144.
Ramsey, C.B., 2009. Bayesian analysis of radiocarbon dates. Radiocarbon 51 (1), 337–360. https://doi.org/10.1017/S0033822200033865.
Perea, Marta Lidia, 2023. Investigaciones en la Parte Superior de la Estructura K-2. In Proyecto Arqueológico Ucanal: Sexta Temporada de Campo, Año 2022, edited by Christina Halperin and Jose Luis Garrido, pp. 45-78, Report Submitted to the Direccion General del Patrimonio Cultural y Natural, Guatemala.
Reed, George F., Freyja Lynn, Meade, Bruce D., 2002. Use of Coefficient of Variation in Assessing Variability of Quantitative Assays. CLIN. DIAGN. LAB. IMMUNOL. 9.
Rice, Prudence, M., 2015. Pottery analysis: a sourcebook. Second edition. University of Chicago Press, Chicago (Ill).
Rytuba, J.J., 2003. Mercury from mineral deposits and potential environmental impact. Environ. Geol.: Int. J. Geosci. 43 (3), 326–338. https://doi.org/10.1007/s00254-002-0629-5.
Sabloff, Jeremy Arac (1944- ...). 2003. Tikal dynasties, foreigners & affairs of state: advancing Maya archaeology. School of American Research advanced seminar series. School of American Research Press ;, Santa Fe.
Salas, Miriam, Jean-Baptiste LeMoine, Jose Luis Garrido, Miguel Angel Cano, Roberto Aguilar, Sheily Hernández, Coloch, Adolto, 2018. Análisis de la Cerámica de Ucanal. In Proyecto Arqueológico Ucanal, 3ra Temporada de Campo, 2017, edited by Christina T. Halperin and José Luis Garrido. Report submitted to the Dirección General del Patrimonio Cultural y Natural, Guatemala City., Guatemala City.

Scarborough, V.L., 1998. Ecology and ritual: water management and the maya. Lat. Am. Antiq. 9 (2), 135–159. https://doi.org/10.2307/971991.

Scarborough, Vernon L., Nicholas P. Dunning, Kenneth B. Tankersley, Christopher Carr, Eric Weaver, Liwy Grazioso, Brian Lane, John G. Jones, Palma Buttles, Fred Valdez, Lentz, David L., 2012. Water and sustainable land use at the ancient tropical city of Tikal, Guatemala. Proc. Natl. Acad. Sci. USA 109(31):12408–12413.

Seefeld, Nicolaus, 2018. The hydraulic system of Uxul: origins, functions, and social setting. Archaeopress pre-Columbian archaeology 9. Archaeopress, Oxford.

Sharer, R.J., Traxler, L.P., Morley, S.G., 2006. The ancient Maya, 6th ed. Stanford University Press, Stanford, Calif.

Suchanek, T.H., Eagles-Smith, C.A., James Harner, E., 2008. Is clear lake methylmercury distribution decoupled from bulk mercury loading. Ecol. Appl. 18 (sp8), A107–A127. https://doi.org/10.1890/06-1649.1.

Takeno, Naoto, 2005. Atlas of Eh-pH diagrams. Intercomparison of thermodynamic databases. National Institute of Advanced Industrial Science and Technology. Research Center for Deep Geological Environments, Japan.

Tankersley, K.B., Dunning, N.P., Carr, C., Lentz, D.L., Scarborough, V.L., 2020. Zeolite water purification at Tikal, an ancient Maya city in Guatemala. Sci. Rep. 10 (1), 18021. https://doi.org/10.1038/s41598-020-75023-7.

Tinkov, A.A., Ajsuvakova, O.P., Skalnaya, M.G., Popova, E.V., Sinitskii, A.I., Nemereshina, O.N., Gatiatulina, E.R., Nikonorov, A.A., Skalny, A.V., 2015. Mercury and metabolic syndrome: a review of experimental and clinical observations. Biometals 28 (2), 231–254. https://doi.org/10.1007/s10534-015-9823-2.

Turner, S., Graham, E., Macphail, R., Duncan, L., Rose, N.L., Yang, H., Whittet, R., Rosique-Esplugas, C., 2021. Mercury enrichment in anthrosols and adjacent coastal sediments at a Classic Maya site, Marco Gonzalez, Belize. *Geoarchaeology* 36 (6), 875–896. https://doi.org/10.1002/gea.21868.

Valdés, J.A., Fahsen, F., 2004. Disaster in Sight: The Terminal Classic at Tikal and Uaxactun. In: The Terminal Classic in the Maya Lowlands: Collapse, Transition, and Transformation, edited by A.A. Demarest, P.M. Rice, and D.S. Rice, pp. 140–161. University Press of Colorado, Boulder.

Vandenabeele, P., Bodé, S., Alonso, A., Moens, L., 2005. Raman spectroscopic analysis of the Maya wall paintings in Ek'Balam, Mexico. Spectrochim. Acta A Mol. Biomol. Spectrosc. 61 (10), 2349–2356. https://doi.org/10.1016/j.saa.2005.02.034.

Wahl, D., Schreiner, T., Byrne, R., Hansen, R., 2007. A Paleoecological Record from a Late Classic Maya Reservoir in the North Petén. Lat. Am. Antiq. 18 (2), 212–222.

Waters, M.N., Brenner, M., Curtis, J.H., Romero-Oliva, C.S., Dix, M., Cano, M., 2021. Harmful algal blooms and cyanotoxins in Lake Amatitlán, Guatemala, coincided with ancient Maya occupation in the watershed. Proc. Natl. Acad. Sci. 118 (48). https://doi.org/10.1073/pnas.2109919118.

Wells, E.C., Terry, R.E., Jacob Parnell, J., Hardin, P.J., Jackson, M.W., Houston, S.D., 2000. Chemical Analyses of Ancient Anthrosols in Residential Areas at Piedras Negras Guatemala. J. Archaeol. Sci. 27 (5), 449–462. https://doi.org/10.1006/jasc.1999.0490.

Whalin, L.M., Mason, R.P., 2006. A new method for the investigation of mercury redox chemistry in natural waters utilizing deflatable Teflon® bags and additions of isotopically labeled mercury. Anal. Chim. Acta 558 (1), 211–221. https://doi.org/10.1016/j.aca.2005.10.070.